Feasibility of ultra-performance liquid chromatography–ion mobility–time-of-flight mass spectrometry in analyzing oxysterols

Petri Kylli[a], Thomas Hankemeier[b,d], Risto Kostiainen[a,*]

[a] Division of Pharmaceutical Chemistry and Technology, Faculty of Pharmacy, University of Helsinki, P.O. Box 56, FI-00014, Finland (linda.ahonen@helsinki.fi, risto.kostiainen@helsinki.fi, petri.kylli@helsinki.fi)

[b] Division of Analytical Biosciences, Leiden Academic Centre for Drug Research, Leiden University, P.O. Box 9502, 2300 RA Leiden, The Netherlands (hankemeier@lacdr.leidenuniv.nl)

[d] Netherlands Metabolomics Centre, Leiden University, P.O. Box 9502, 22300 RA Leiden, The Netherlands (hankemeier@lacdr.leidenuniv.nl)

*Corresponding author, e-mail: risto.kostiainen@helsinki.fi

Abstract

Oxysterols are oxygenated cholesterols that are important in many cell functions and they may also be indicative of certain diseases. The purpose of this work was to study the feasibility of ultra-performance liquid chromatography–ion mobility–time-of-flight mass spectrometry (UPLC–IM–TOFMS) using traveling wave cell in analyzing oxysterols and especially their isomers in biological samples. . Oxysterols were analyzed as their *p*-toluenesulfonyl isocyanate derivatives, which improved the separation of isomeric oxysterols by ion mobility and ionization efficiency in the electrospray ionization step. The UPLC–IM–TOFMS method was shown to be fast and to provide good quantitative performance. The feasibility of the method was demonstrated in the analyses of oxysterols in fibroblast cell samples.

Key words

liquid-chromatography-ion-mobility-mass-spectrometry,oxysterol, oxysterol Isomers, derivatization, fibroblast cell samples

Introduction

Oxysterols are oxygenated cholesterols that are either formed by cholesterol hydroxylases that belong to the cytochrome P450 family [1-3] or by auto-oxidation [4]. Oxysterols are involved in various biological events such as cholesterol homeostasis, apoptosis, cell differentiation, and signaling [5-8]. The most abundant oxysterols are 24(*S*)-, 27- and 7α-hydroxycholesterols in human serum [9]. The formation of 24(*S*)-hydroxycholesterol is catalyzed by CYP46A1 in the brain whereas 27- and 7α-hydroxycholesterols are catalyzed by CYP27A1 and CYP7A1 in the liver [10, 11]. 24(*S*)- and 27-hydroxycholesterols have been linked with several neurodegenerative diseases such as Alzheimer's disease and Parkinson's disease [12, 13]. Elevated levels of 24(*S*)-hydroxychloesterol have been detected in samples of cerebrospinal fluid taken from patients that suffer from Alzheimer's disease [12]. Though oxysterols have been linked with diseases, they are also part of normal cholesterol metabolism. Cholesterol in the brain is converted into 24(*S*)-hydroxycholesterol, which can permeate across the blood brain barrier into the circulation [14]. Recently, it has been shown that oxysterols have a role in dopaminergic neurogenesis [15]. The addition of exogenous 22-hydroxycholesterol caused a 2-fold increase in dopaminergic neurogenesis in mouse embryo cells compared to controls [15]. Oxysterols, such as 22(*R*)-hydroxycholesterol, 20(*S*)-hydroxycholesterol, and 22(*S*)-hydroxycholesterol induced alkaline phosphatase activity, which is an early marker of osteogenic differentiation [16, 17].

Highly sensitive and selective analytical methods are needed for the analysis oxysterols in complex biological samples. The gold standard for the analysis of oxysterols is gas chromatography–mass spectrometry (GC–MS) [18-21], which is performed after derivatization of the oxysterols. One such derivatization is by trimethylsilylation, which makes them more volatile and thermally stable for the analysis. Liquid chromatography–mass spectrometry (LC-MS) [22], with electrospray ionization (ESI) [23, 24] or atmospheric pressure chemical ionization (APCI) [25] or atmospheric pressure photoionization (APPI) [26] has been increasingly used for the analysis of oxysterols. Although APCI [25] and APPI [26] provide high ionization efficiency for non-derivatized oxysterols, ESI is the preferred method due to its superior sensitivity for derivatized oxysterols [27]. Several derivatization procedures have been used for the LC–ESI–MS analysis of oxysterols such as derivatization to picolinyl esters, nicotinyl esters, N,N-dimethylglycine esters, oximes, and Girard hydrazones [22]. In addition to its high sensitivity, the high separation power of the chromatographic method is needed in order to separate different isomeric oxysterols, which is not possible by mass spectrometry alone because the

fragmentation behaviour of isomeric oxysterols are very similar. The separation of oxysterols is possible with GC [21] and LC [23]. However, the separation of isomeric oxysterols require relatively long run times, which significantly increase the total analyses times. Therefore, faster analytical methods are needed for the determination and analysis of oxysterols in order to increase sample throughput.

Ion mobility–mass spectrometry (IM–MS) is a powerful tool in bioanalysis and it has been increasingly used along with the development of commercial instruments. For example, IM-MS is used in metabolomics, in proteomics and in targeted analysis [28-30]. IM–MS provides high sensitivity, high specificity and analysis times that can be measured on millisecond timescales. Analytes are separated by IM–MS in the gas phase when traveling through a drift gas (normally N_2) with a velocity that is dependent on the charge, shape, size, polarity, and collision cross section (CCS) of the analyte [29, 31]. The CCS provides an additional identification parameter in IM–MS in addition to the drift time, the *m/z* value and fragmentation pattern and it can be estimated by calibrating the IMS using compounds with known CCSs. The IM combined with LC–MS is also increasingly used in bioanalytics [32-34], because IM provides an additional degree of separation and thus significantly improved peak capacity and specificity. This can be particularly beneficial for example in the analysis of complex biological samples and in the separation of isomeric compounds [35, 36].

The recently introduced traveling wave ion mobility (TWIM) provides a new mode of ion separation prior MS analysis. In TWIM ions are accumulated in the trap cell and released into the mobility cell by continuous voltage pulses providing high ion transmission and good separation efficiency [37]. The TWIM–MS provides high sensitivity, specificity, and analysis times on a millisecond timescale and the method has been increasingly used in bioanalytical applications [38-40].

In this study we have investigated for the first time the feasibility of UPLC–TWIM–TOFMS in the analysis of oxysterols. The oxysterols were derivatized by *p*-toluenesulfonyl isocyanate (PTSI) in order to increase the respective CCS, which thus increases the separation power of IM and enhances ionization efficiency of oxysterols in electrospray ionization (ESI). PTSI derivatization was selected as the method, which has been applied successfully earlier for the separation of steroid isomers by TWIM [33]. The aim of the study was to improve sample throughput by using UPLC–TWIM–TOFMS that provides improved separation efficiency and thus faster analysis of oxysterol isomers than commonly used LC-MS or GC-MS methods. Furthermore, we have investigated the feasibility of the UPLC–TWIM–TOFMS method in quantitative analysis of oxysterols in fibroblast cell samples.

Materials and methods

Chemicals

Ultra LC–MS grade methanol (MeOH) and acetonitrile (ACN) were purchased from Actu-All Chemicals (Oss, The Netherlands). Water was purified using a Millipore Milli-Q Gradient A10 purification system (Molsheim, France). 22-hydroxycholesterol (22-OH-chl, cholest-5-ene-3β,22-diol, 7α-hydroxycholesterol (7α-OH-chl, 5-cholesten-3β,7α-diol) and 7β-hydroxycholesterol (7β-OH-chl, 5-cholesten-3β,7β-diol) were purchased from Fountain Limited (Naxxar, Malta), 24*(S)*-hydroxycholesterol (24(*S*)-OH-chl, cholest-5-ene-3β,24α-diol) from AH diagnostics Oy (Helsinki, Finland), 27-hydroxycholesterol (27-OH-chl, cholest-5-ene-3β,26-diol) from Santa Cruz Biotechnology, Inc. (Heidelberg, Germany) and 7-ketocholesterol (7-ketochl, 3β-hydroxy-5-cholesten-7-one) and 27-hydroxycholesterol-d6 (d6-27-OH-Chl, 25,26,26,26,27,27-hexadeuterocholest-5-ene-3,27-diol) from Avanti Polar Lipids (Alabaster, AL, USA). The *p*-toluenesulfonyl isocyanate (PTSI, 96%), poly-DL-alanine and analytical grade ammonium acetate (99%) were purchased from Sigma-Aldrich (St. Louis, MO, USA).

Sample preparation and derivatization

A stock solution (1 mg mL^{-1}) of each standard compound used was prepared by dissolving it in methanol. Further dilutions of working solutions were also prepared in methanol. A sample or working standard solution in a vial was evaporated to dryness under nitrogen flow. The derivatization reaction was performed according to the method described by Zuo et al. [41]. A 100 µL volume of ACN was added to the vial followed by 20 µL of PTSI solution (100 µL mL^{-1} in ACN). The solution in the vial was agitated by a vortex mixer for 2 min and the reaction was stopped by adding 20 µL of H_2O. The PTSI derivatization reaction is shown in Fig. S1 and the PTSI derivatized oxysterols used in this study are shown in Fig. S2.

Newborn human foreskin fibroblasts (ATCC, CRL-2429) were cultured in Dulbecco's modified Eagle's medium (DMEM) with glutamine, 10% fetal bovine serum (Gibco, Carlsbad, CA, USA), and 1% mixture of penicillin, streptomycin, fungizone (Gibco), and incubated in a CO_2 incubator (5% CO_2) at 37°C. Fibroblasts were cultured in T-165 flasks. The medium was removed and the cells were washed twice with phosphate buffered saline. Subsequently, MeOH:H_2O (50:50) was added to the cells, collected in a tube, sonicated for 10 minutes and centrifuged at 10 000g for 10 minutes. The supernatant was removed

and the pellet was then extracted in triplicate by adding 0.5 mL cyclohexane:ethyl acetate (3:1) containing 7 ng mL^{-1} of d6-27-OH-Chl as an internal standard to the Eppendorf tubes, then vortex mixing and sonicating each replicate in an ultrasonic bath for 15 min. The Eppendorf tubes were centrifuged at 4°C and 13 200 rpm (19500 rfc) for 10 min. The supernatant was transferred to a new Eppendorf tube. The remaining cell pellet was re-extracted with 0.5 mL of cyclohexane:ethyl acetate (3:1) in the ultrasonic bath and centrifuged as described above. After centrifugation the supernatants were combined and extracted with 200 µL of H_2O. The organic layer was saved and evaporated to dryness in a SpeedVac evaporator. The derivatization was performed as described above.

UPLC–IM–TOFMS

A Waters Synapt G2-S Q-TOF HDMS (Waters, Wilmslow, UK) mass spectrometer equipped with a traveling wave ion mobility cell was used in the IM–MS analysis. The mass spectrometer was operated in negative ion ESI mode using the resolution of 20000 FWHM. Capillary voltage was 2.5 kV, source temperature 120 °C, desolvation temperature 450 °C, desolvation gas flow 800 L h^{-1} and nebulizer gas pressure 6.0 bar. Sampling cone voltage was set to 40 V and source offset to 80 V. The acquisition mass range was *m/z* 50-1200.

The optimization of the method and the acquisition of the mass spectra of the analytes were acquired by direct infusion of standard sample solution (derivatized oxysterols in ACN) at the flow rate of 10 µL min^{-1}. The infusion flow was combined with the flow (400 µL min^{-1}) of 10 mM ammonium acetate in MeOH from a Waters UPLC binary solvent manager before the ion source.

A Waters Acquity UPLC (Waters) was used in the analysis of oxysterols by UPLC–IM–TOFMS. The column was Waters Acquity BEH C18, (2.1 x 100 mm, 1.7 µm) and the column temperature was 45 °C. Milli-Q water (A) and 10 mM ammonium acetate in methanol (B) were used as the mobile phases for the gradient elution. The gradient was 0-1 min 50% B → 100% B, 1-3 min 100% B, and equilibration with 50% of B for 2 min. The flow rate was 0.4 mL min^{-1} and the injection volume was 5 µL. The samples were injected using a Waters UPLC sample manager.

The optimal settings for the TWIM cell were the following: helium cell gas flow rate: 180 mL min^{-1}, IM cell gas flow rate: 90 mL min^{-1} (3.0 mbar), IM wave height: 40.0 V, and IM wave velocity linear ramp 300-1000 m s^{-1}. The IM buffer gas was nitrogen.

The effect of the N_2 buffer gas pressure (2.5-3.5 mbar) was studied. The peak-to-peak (R_{p-p}) resolutions of the adjacent peaks were calculated according to equations presented in Supplementary material. The CCS of the analytes were determined using 10 µg mL^{-1} poly-DL-alanine as a calibrant. The calibration curves were plotted according to TWIM CCS values of poly-DL-alanine molecules in the literature [42]. The CCS values and the concentrations in the quantitative analytes were determined from driftograms using Driftscope software.

Results and discussion

The oxysterol isomers were not separated in their native forms by IM because they had very similar CCSs and also due to having similar strengths of their ion-molecule interactions with the drift gas. The ionization efficiency of oxysterols with ESI was relatively poor as they lack an ionic group and their proton affinities were relatively low due to their nonpolar character. The PTSI derivatization of the oxysterols improved the separation efficiency due to their increased ion-molecule interactions and CCSs. The derivatization also improved the ionization efficiency and all the derivatives produced very intense deprotonated molecule with minimal fragmentation and provided good sensitivity in the IM–MS analysis.

The effect of drift gas (N_2) pressure (2.5, 3.0, and 3.5 bar) on ion mobility separation efficiency was studied by using selected positional isomers of PTSI-derviatized oxysterols, namely: the PTSI-derivatives of 22-OH-, 24(*S*)-OH- and 27-OH-cholesterols (Fig. S3). At every chosen pressure setting 22-OH-cholesterol was fully separated from 24(*S*)-OH- and 27-OH-cholesterols, but 24(*S*)-OH- and 27-OH-cholesterols were only partly separated from each other (Figure 3). At pressures of 2.5, 3.0, and 3.5 bar the respective R_{p-p} between 22-OH- and 24(*S*)-OH-cholesterols were 0.54, 0.93, and 1.25, whereas between 24(*S*)-OH- and 27-OH-cholesterols the corresponding R_{p-p} were 0.54, 0,54 and 0.46. The results show that the resolution between 22-OH- and 24(*S*)-OH-cholesterols increased when the pressure of N_2 was raised, although the resolution between 24(*S*)-OH- and 27-OH-cholesterols did not change significantly. On the other hand, the sensitivity was decreased by about 4-fold when the pressure was increased from 2.5 bar to 3.5 bar but decreased only by about 1.5-fold when the pressure was increased from 2.5 bar to 3.0 bar. The decreased sensitivity at higher drift gas pressures is due to the decreased ion transmission through the TWIM cell. The drift gas pressure of 3.0 bar provided the best compromise between resolution and sensitivity based on these results.

The drift times and collision cross sections of the PTSI derivatives of the six studied oxysterols are presented in Table 1. The CCS was 274.26 $Å^2$ for 7-ketocholesterol and between 284.14 and 309.34 $Å^2$ for the other oxysterols. The CCS of 7-ketocholesterol was smaller because it produced a mono-PTSI derivate whereas the other oxysterols have two hydroxyl groups to produce di-PTSI-derivatives. Thus, 7-ketocholesterol was well separated from the other oxysterols. A more branched structure causes a larger collision cross section in 7α-OH-, 7β-OH- and 22-OH-cholesterols than in 24(*S*)-OH- and 27-OH-cholesterols where the site of the derivatization is at the end of the side-chain (Fig. S2). The PTSI-derivatized oxysterols 22-OH-, 24(*S*)-OH-, 27-OH-cholesterols were at least partly separated from each other (Fig. 1A). Both 7α-OH- and 7β-OH-cholesterol standards, when analyzed separately, showed two peaks in their selected mobility traces (Fig. S4 B and C) that is obviously due to formation of two protomers. The same was not observed with other oxysterols. It seems that the derivatized oxysterols having both PTSI groups at the ring structure (carbon 3 and 7) favors separation of protomers compared to the oxysterols having other PTSI group at carbon 3 and other at the side chain. When 7α-OH- and 7β-OH-cholesterol standards were analyzed as a mixture, the protomer 1 of 7α-OH-cholesterol was separated but the protomer 2 of 7α-OH-cholesterol and the protomers 1 and 2 of 7β-OH-cholesterol overlapped and were not separated from each other (Fig. 1 and Fig. S 4A). Furthermore, the protomers of 7α-OH- and 7β-OH-cholesterol anomers overlapped with the 24(*S*)-OH- and 22-OH-cholesterols (Fig. 1). These results show that the separation power of IM alone is insufficient for full separation of all the oxysterols and more specific methods are needed.

UPLC–IM–TOFMS of fibroblast cell samples

The UPLC was interfaced with the IM–TOFMS in order to improve the specificity in the analysis of the oxysterols. The 2-D separation map of $[M-H]^-$ ions (m/z 796.3791 +/- 10 ppm) (Fig. 2) shows that the PTSI derivatives of 22-OH-, 24(*S*)-OH-, 27-OH-cholesterols were separated from 7α-OH-, 7β-OH-cholesterols by UPLC–IM–TOFMS that was not possible by IM–TOFMS alone. Similar to that found for the IM–TOFMS analysis, the the protomer 1 of 7α-OH-cholesterol was separated, but the protomer 2 of 7α-OH-cholesteroloverlapped with 7β-OH-cholesterol protomers (Fig. 2). Therefore, the peak areas of 7α-OH- and 7β-OH cholesterols were summarized in quantitative analysis. However, it is possible to estimate the concentrations of 7α-OH- and 7β-OH-cholesterol separately based on the separated peak of

the protomer 1 of 7α-OH-cholesterol. The peak area of the protomer 1 of 7α-OH cholesterol is 25% of the peak area of the protomer 2 of 7α-OH cholesterol (Fig. 4S) that provides estimation of the total concentration of 7α-OH-cholesterol in quantitative analysis. When the estimated peak area of protomer 2 of 7α-OH-cholesterol is subtracted from the overlapping peak of the protomer 2 of 7α-OH-cholesterol and the protomers 1 and 2 of 7β-OH-cholesterol the total concentration of 7β-OH-cholesterol can be estimated. However, the repeatability of the formation of the protomers must be studied in more detail before this estimation can be utilized in quantitative analysis of 7α-OH- and 7β-OH-cholesterols. The analysis of 7-ketocholesterol was not a problem, since it separated well from other oxysterols by UPLC–IM and it appeared at a different *m/z* ratio than other oxysterols. The improved specificity owing to IM allowed to use fast gradients in UPLC separation that significantly shortened the separation times (about 2 min) compared to the LC-MS methods (7-15 min) presented in the literature [20-25].

The quantitative performance of analysis of UHPLC–IMS–MS in the analysis of oxysterols was studied with respect to the limits of detection (LOD), the limits of quantification (LOQ), linearity, and intra- and inter-day repeatability. The LODs (at S/N ≥3) were 0.5-1.0 ng mL^{-1} and LOQs 1.0-5.0 ng mL^{-1}, which indicates good sensitivity for the method. Linearity of the calibration curves and intra- and inter-day repeatabilities were determined using analyte to d6-27-OH-Chl internal standard (ISTD) peak area ratios. Calibration curves were determined using the linear regression with 1/X weighting within a concentration range of 0.5 – 250 ng mL^{-1}. The coefficients of determination (R^2) for the calibration curves were better than 0.995 for all the compounds and thus acceptable. Five replicate injections of 10 ng mL^{-1} of standard sample were made for intra- and inter-day repeatability tests. The relative standard deviations (%RSD) for intra-day and inter-day repeatabilities for the analyte/ISTD peak area ratios were below 8% and 19%, respectively, which indicate acceptable levels of repeatability. These results show good quantitative performance of the method for the analysis oxysterols.

The feasibility of the UPLC–IM–TOFMS method for the analysis of biological samples was studied by quantifying oxysterols in fibroblast cell samples that contained four million cells (Fig. 2B). The use of high resolution mass spectrometry with a mass window of 10 ppm ensured the specific analysis of the selected oxysterols without significant background disturbances from the sample matrix. All six compounds, 22-OH-, 24(*S*)-OH-, 27-OH-, 7-OH-cholesterols and 7-ketocholesterol, were detected in the fibroblast cell samples (Table 3, Fig 2B). The concentrations of 7α-OH- + 7β-OH-cholesterols and 7-ketocholesterol were 47.8 ng mL^{-1} and 5.9 ng mL^{-1} (1.67 and 0.21 ng/million cells, respectively). These

compounds were clearly detected with good repeatability in three replicate analysis. The 22-OH-, 24(*S*)-OH-, 27-OH-cholesterols were also detected but their concentrations were below the LOQ but above LOD. It can be estimated, however, that the concentrations of 22-OH-oxysterols in the cell samples were between 0,5 – 1 ng mL^{-1} (0.018 – 0.035 ng/million cells) and the concentrations of 24(S)-OH- and 27-OH-oxysterols between 1-5 ng mL^{-1} (0.035 – 0.18 ng/million cells).

Conclusions

The separation of isomeric oxysterols is of high importance as it facilitates getting more detailed and therefore useful information on the role of oxysterols in biological systems. We showed that UPLC–IM–TOFMS provides a potentially useful and reliable method for the analysis of oxysterols in biological samples. The PTSI-derivatization of oxysterols improves separation of isomeric oxysterols in addition to improving their ionization efficiencies in electrospray ionization. However, the full separation of isomeric oxysterols was not possible solely by IM and the combination of UPLC–IM was needed in order to enhance separation efficiency. However, the partial separation of isomeric oxysterols by IM made possible to use rapid gradients in UPLC in order to achieve fast analysis with acceptable separation. The method was shown to provide acceptable quantitative performance and its feasibility was successfully demonstrated in the analyses of six oxysterols in fibroblast cell samples.

Acknowledgements

We gratefully acknowledge the Finnish Funding Agency for Innovation (Tekes) large strategic research opening project no. 40395/13 for financial support.

References

[1] V. Mutemberezi, O. Guillemot-Legris, G.G. Muccioli, Oxysterols: From cholesterol metabolites to key mediators, Progress in Lipid Research, 64 (2016) 152-169.
[2] I.A. Pikuleva, Cholesterol-metabolizing cytochromes P450, Drug Metab Dispos, 34 (2006) 513-520.
[3] I. Björkhem, Five decades with oxysterols, Biochimie, 95 (2013) 448-454.
[4] G.J. Schroepfer, Oxysterols: Modulators of cholesterol metabolism and other processes, Physiological Reviews, 80 (2000) 361-554.
[5] R. Kuver, Mechanisms of oxysterol-induced disease: insights from the biliary system, Clinical Lipidology, 7 (2012) 537-548.
[6] V.M. Olkkonen, O. Béaslas, E. Nissilä, Oxysterols and Their Cellular Effectors, Biomolecules, 2 (2012).
[7] J. Makoukji, G.G. Shackleford, D. Meffre, J. Grenier, P. Liere, J.-M.A. Lobaccaro, M. Schumacher, C. Massaad, Interplay between LXR and Wnt/beta-Catenin Signaling in the Negative Regulation of Peripheral Myelin Genes by Oxysterols, Journal of Neuroscience, 31 (2011) 9620-9629.
[8] N.J. Spann, C.K. Glass, Sterols and oxysterols in immune cell function, Nat Immunol, 14 (2013) 893-900.

[9] V.V.R. Bandaru, N.J. Haughey, Quantitative detection of free 24S-hydroxycholesterol, and 27-hydroxycholesterol from human serum, BMC Neuroscience, 15 (2014) 1-9.
[10] I. Bjorkhem, Rediscovery of cerebrosterol, Lipids, 42 (2007) 5-14.
[11] P.V. Luoma, Cytochrome P450 - Physiological key factor against cholesterol accumulation and the atherosclerotic vascular process, Annals of Medicine, 39 (2007) 359-370.
[12] P. Schonknecht, D. Lutjohann, J. Pantel, H. Bardenheuer, T. Hartmann, K. von Bergmann, K. Beyreuther, J. Schroder, Cerebrospinal fluid 24S-hydroxycholesterol is increased in patients with Alzheimer's disease compared to healthy controls, Neuroscience Letters, 324 (2002) 83-85.
[13] I. Bjorkhem, M. Heverin, V. Leoni, S. Meaney, U. Diczfalusy, Oxysterols and Alzheimer's disease, Acta neurologica Scandinavica. Supplementum, 185 (2006) 43-49.
[14] D. Lütjohann, K. Von Bergmann, 24S-Hydroxycholesterol: A Marker of Brain Cholesterol Metabolism, Pharmacopsychiatry, 36 (2003) S102-S106.
[15] P. Sacchetti, K.M. Sousa, A.C. Hall, I. Liste, K.R. Steffensen, S. Theofilopoulos, C.L. Parish, C. Hazenberg, L. Auml;hrlund-Richter, O. Hovatta, J.A. Gustafsson, E. Arenas, Liver X Receptors and Oxysterols Promote Ventral Midbrain Neurogenesis In Vivo and in Human Embryonic Stem Cells, Cell Stem Cell, 5 (2009) 409-419.
[16] H.T. Kha, B. Basseri, D. Shouhed, J. Richardson, S. Tetradis, T.J. Hahn, F. Parhami, Oxysterols regulate differentiation of mesenchymal stem cells: Pro-bone and anti-fat, Journal of Bone and Mineral Research, 19 (2004) 830-840.
[17] T.L. Aghaloo, C.M. Amantea, C.M. Cowan, J.A. Richardson, B.M. Wu, F. Parhami, S. Tetradis, Oxysterols enhance osteoblast differentiation in vitro and bone healing in vivo, Journal of Orthopaedic Research, 25 (2007) 1488-1497.
[18] W.J. Griffiths, Y. Wang, Analysis of oxysterol metabolomes, Biochimica et Biophysica Acta (BBA) - Molecular and Cell Biology of Lipids, 1811 (2011) 784-799.
[19] H.-F. Schoett, D. Luetjohann, Validation of an isotope dilution gas chromatography-mass spectrometry method for combined analysis of oxysterols and oxyphytosterols in serum samples, Steroids, 99 (2015) 139-150.
[20] W.J. Griffiths, P.J. Crick, Y. Wang, Methods for oxysterol analysis: Past, present and future, Biochem Pharmacol, 86 (2013) 3-14.
[21] S. Dzeletovic, O. Breuer, E. Lund, U. Diczfalusy, Determination of Cholesterol Oxidation Products in Human Plasma by Isotope Dilution-Mass Spectrometry, Anal Biochem, 225 (1995) 73-80.
[22] W.J. Griffiths, J. Abdel-Khalik, P.J. Crick, E. Yutuc, Y. Wang, New methods for analysis of oxysterols and related compounds by LC-MS, J. Steroid Biochem. Mol. Biol., (2015) Ahead of Print.
[23] J.G. McDonald, D.D. Smith, A.R. Stiles, D.W. Russell, A comprehensive method for extraction and quantitative analysis of sterols and secosteroids from human plasma, J Lipid Res, 53 (2012) 1399-1409.
[24] Z. Pataj, G. Liebisch, G. Schmitz, S. Matysik, Quantification of oxysterols in human plasma and red blood cells by liquid chromatography high-resolution tandem mass spectrometry, J. Chromatogr. A, 1439 (2016) 82-88.
[25] V. Mutemberezi, J. Masquelier, O. Guillemot-Legris, G.G. Muccioli, Development and validation of an HPLC-MS method for the simultaneous quantification of key oxysterols, endocannabinoids, and ceramides: variations in metabolic syndrome, Anal Bioanal Chem, 408 (2016) 733-745.
[26] L. Ahonen, F.B.R. Maire, M. Savolainen, J. Kopra, R.J. Vreeken, T. Hankemeier, T. Myohanen, P. Kylli, R. Kostiainen, Analysis of oxysterols and vitamin D metabolites in mouse brain and cell line samples by ultra-high-performance liquid chromatography-atmospheric pressure photoionization-mass spectrometry, J. Chromatogr. A, 1364 (2014) 214-222.
[27] A. Honda, K. Yamashita, T. Hara, T. Ikegami, T. Miyazaki, M. Shirai, G. Xu, M. Numazawa, Y. Matsuzaki, Highly sensitive quantification of key regulatory oxysterols in biological samples by LC-ESI-MS/MS, J Lipid Res, 50 (2009) 350-357.
[28] G. Paglia, M. Kliman, E. Claude, S. Geromanos, G. Astarita, Applications of ion-mobility mass spectrometry for lipid analysis, Anal Bioanal Chem, 407 (2015) 4995-5007.

[29] C. Lapthorn, F. Pullen, B.Z. Chowdhry, Ion mobility spectrometry-mass spectrometry (IMS-MS) of small molecules: Separating and assigning structures to ions, Mass Spectrom. Rev., 32 (2013) 43-71.
[30] Y. Zhong, S.-J. Hyung, B.T. Ruotolo, Ion mobility-mass spectrometry for structural proteomics, Expert Rev. Proteomics, 9 (2012) 47-58.
[31] F. Lanucara, S.W. Holman, C.J. Gray, C.E. Eyers, The power of ion mobility-mass spectrometry for structural characterization and the study of conformational dynamics, Nat. Chem., 6 (2014) 281-294.
[32] C.W.N. Damen, G. Isaac, J. Langridge, T. Hankemeier, R.J. Vreeken, Enhanced lipid isomer separation in human plasma using reversed-phase UPLC with ion-mobility/high-resolution MS detection, J Lipid Res, 55 (2014) 1772-1783.
[33] T. Pacini, W. Fu, S. Gudmundsson, A.E. Chiaravalle, S. Brynjolfson, B.O. Palsson, G. Astarita, G. Paglia, Multidimensional Analytical Approach Based on UHPLC-UV-Ion Mobility-MS for the Screening of Natural Pigments, Analytical Chemistry, 87 (2015) 2593-2599.
[34] A. Thomas, W. Schaenzer, M. Thevis, Determination of human insulin and its analogues in human blood using liquid chromatography coupled to ion mobility mass spectrometry (LC-IM-MS), Drug Test. Anal., 6 (2014) 1125-1132.
[35] L. Ahonen, M. Fasciotti, G.B. af Gennas, T. Kotiaho, R.J. Daroda, M. Eberlin, R. Kostiainen, Separation of steroid isomers by ion mobility mass spectrometry, Journal of Chromatography A, 1310 (2013) 133-137.
[36] E. Reading, J. Munoz-Muriedas, A.D. Roberts, G.J. Dear, C.V. Robinson, C. Beaumont, Elucidation of Drug Metabolite Structural Isomers Using Molecular Modeling Coupled with Ion Mobility Mass Spectrometry, Anal. Chem. (Washington, DC, U. S.), 88 (2016) 2273-2280.
[37] A.A. Shvartsburg, R.D. Smith, Fundamentals of Traveling Wave Ion Mobility Spectrometry, Analytical chemistry, 80 (2008) 9689-9699.
[38] A.B. Kanu, P. Dwivedi, M. Tam, L. Matz, H.H. Hill, Ion mobility-mass spectrometry, Journal of Mass Spectrometry, 43 (2008) 1-22.
[39] P.M. Lalli, B.A. Iglesias, H.E. Toma, G.F. de Sa, R.J. Daroda, J.C. Silva, J.E. Szulejko, K. Araki, M.N. Eberlin, Protomers: formation, separation and characterization via travelling wave ion mobility mass spectrometry, Journal of Mass Spectrometry, 47 (2012) 712-719.
[40] G.A. Bataglion, G.H. Martins Ferreira Souza, G. Heerdt, N.H. Morgon, J.D. Lisboa Dutra, R.O. Freire, M.N. Eberlin, A. Tata, Separation of glycosidic catiomers by TWIM-MS using CO2 as a drift gas, Journal of Mass Spectrometry, 50 (2015) 336-343.
[41] M. Zuo, M.-j. Gao, Z. Liu, L. Cai, G.-L. Duan, p-Toluenesulfonyl isocyanate as a novel derivatization reagent to enhance the electrospray ionization and its application in the determination of two stereo isomers of 3-hydroxyl-7-methyl-norethynodrel in plasma, Journal of Chromatography B, 814 (2005) 331-337.
[42] J.G. Forsythe, A.S. Petrov, C.A. Walker, S.J. Allen, J.S. Pellissier, M.F. Bush, N.V. Hud, F.M. Fernandez, Collision cross section calibrants for negative ion mode traveling wave ion mobility-mass spectrometry, Analyst, 140 (2015) 6853-6861.

Figures

Figure 1. Selected ion mobility responses of the $[M-H]^-$ ions (*m/z* 795.3718 +/- 10 ppm) of the PTSI-derivatized A) 22-, 24(*S*)- and 27-OH-cholesterol and B) 7α-OH- and 7β-OH-cholesterol.

Figure 2. 2-D separation map of the $[M-H]^-$ ions (m/z 796.3791 +/- 10 ppm) of 22-OH-, 24(S)-OH-, 27-OH-, and 7α-OH-/7β-OH-cholesterols of A) standard sample (2 ng mL^{-1}) and B) fibroblast sample (4 million cells) by UPLC–IM–TOFMS. P1 = protomer 1 and P2 = protomer 2.

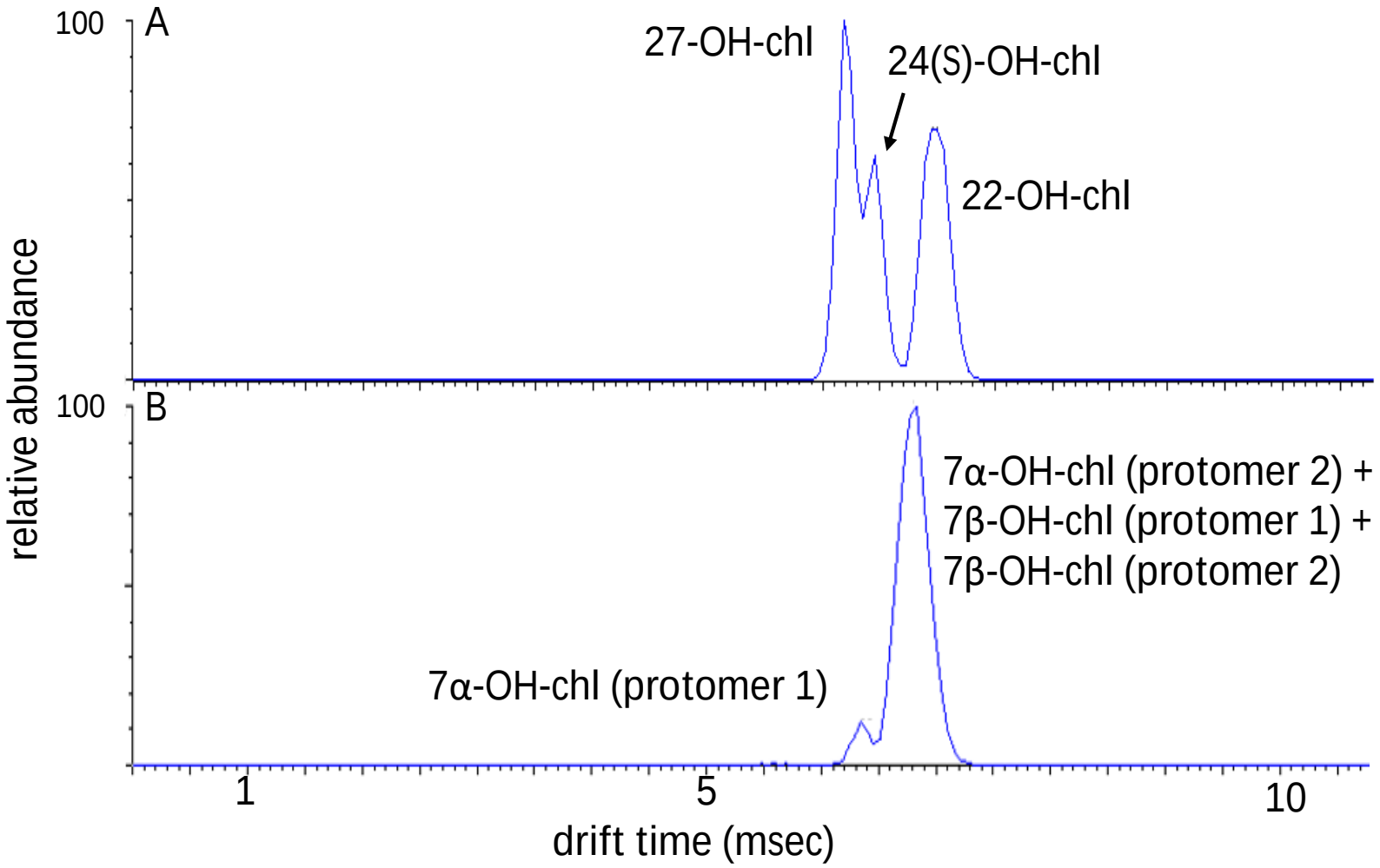
100
A
27-OH-chl
24(S)-OH-chl
22-OH-chl
100
B
7α-OH-chl (protomer 2) +
7β-OH-chl (protomer 1) +
7β-OH-chl (protomer 2)
7α-OH-chl (protomer 1)
relative abundance
1
5
10
drift time (msec)

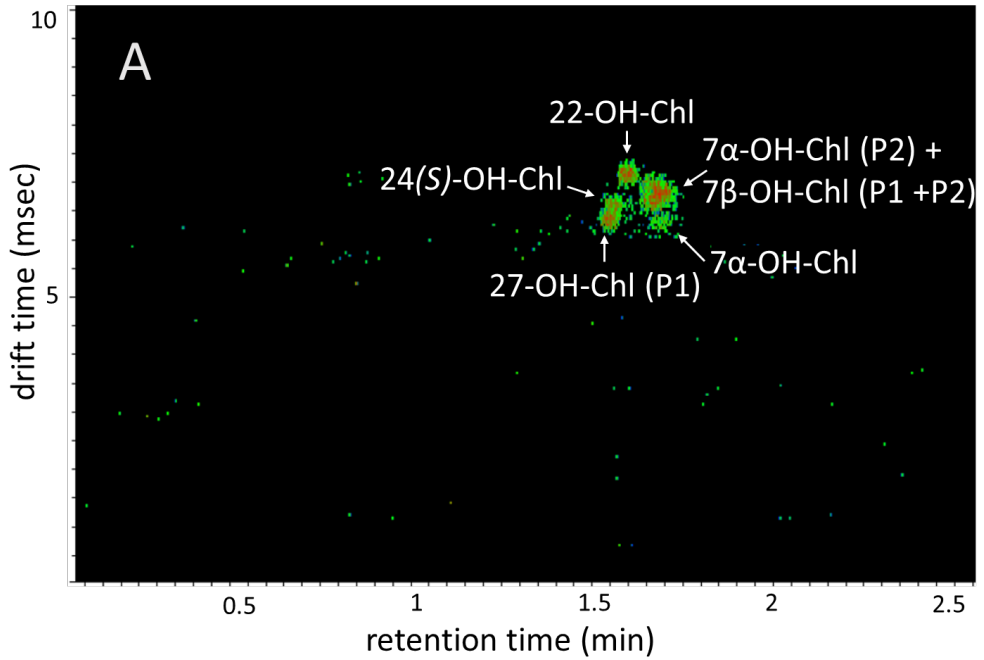
A
22-OH-Chl
7α-OH-Chl (P2) +
7β-OH-Chl (P1 +P2)
24(S)-OH-Chl
7α-OH-Chl
27-OH-Chl (P1)
drift time (msec)
10
5
0.5
1
1.5
2
2.5
retention time (min)

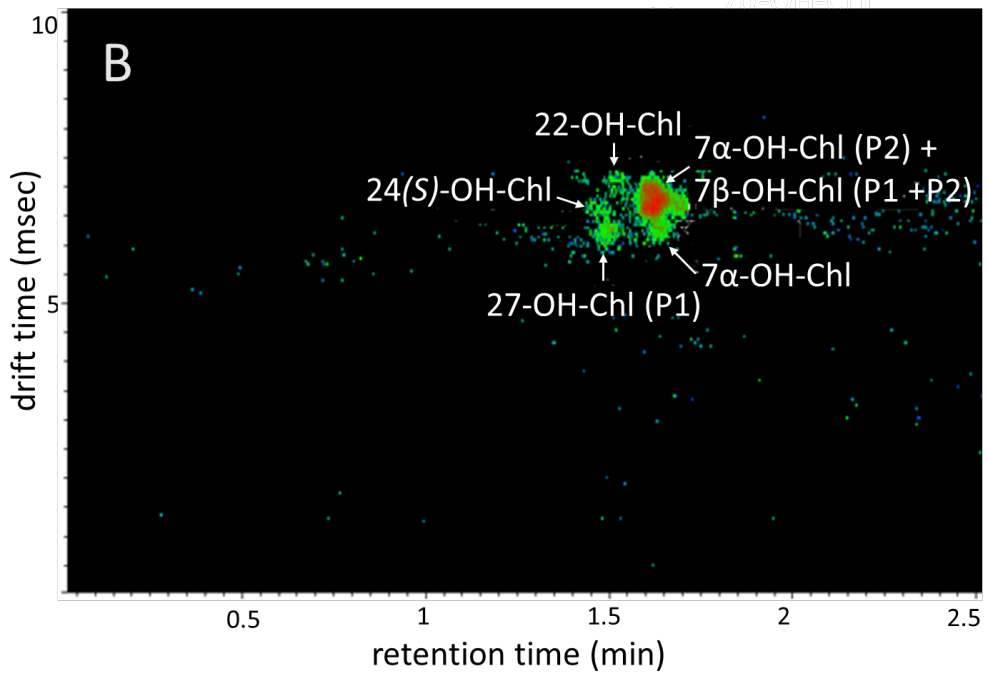
B
22-OH-Chl
7α-OH-Chl (P2) +
7β-OH-Chl (P1 +P2)
24(S)-OH-Chl
7α-OH-Chl
27-OH-Chl (P1)
drift time (msec)
10
5
0.5
1
1.5
2
2.5
retention time (min)

Table 1. IM–TOFMS data of the oxysterols

Compound	m/z value $[M-H]^-$	Drift time (msec)	CCS value ($Å^2$)
7α-OH-Chl	795.3718	6.47 (P1), 6.94 (P2)	291.87 (P1), 306.21 (P2)
7β-OH-Chl	795.3718	6.68 (P1), 7.00 (P2)	298.35 (P1), 308.05 (P2)
22-OH-Chl	795.3718	7.03	309.34
24(S)-OH-Chl	795.3718	6.47	291.87
27-OH-Chl	795.3718	6.34	284.00
7-ketochl	596.3415	5.87	274.26
d6-27-OH-Chl*	801.4095	6.22	284.14

P1 = protomer 1, P2 = protomer 2

Table 2. Limits of detection (LOD), limits of quantification (LOQ), coefficients of determination (R^2), intra- and inter-day repeatability of the analysis

Compound	LOD (ng mL^{-1})	LOQ (ng mL^{-1})	R^2 (range, ng mL^{-1})	$\%RSD_{intra}$ (N = 5)	$\%RSD_{inter}$ (N = 15, 3 x 5)
22-OH-Chl	0.5	1.0	0.9985 (1.0-200)	5.13	14.79
24(S)-OH-Chl	1.0	5.0	0.9953 (5.0-150)	2.90	13.02
27-OH-Chl	1.0	5.0	0.9963 (5.0-200)	1.54	15.83
7α-OH-Chl (P1)*	1.0	3.0	0.9853 (3.0-150)	5.60	18.40
7α-OH-Chl (P2)* + 7β-OH-Chl (P1, P2)*	1.0	3.0	0.9957 (3.0-200)	7.42	14.99
7-ketochl	0.5	1.5	0.9974 (1.5-200)	3.64	14.45

* P1 = protomer 1, P2 = protomer 2.

Table 3. Concentrations of oxysterols in fibroblast cell samples (four million cells). The analysis were carried out with three repetitive runs.

Compound	Concentration	
	(ng mL^{-1} , mean ± SD)	(ng/million cells ± SD)
22-OH-Chl	0.5 – 1.0 (>LOD < LOQ)	0.018 – 0.035
24(S)-OH-Chl	1.0 – 5.0 (>LOD < LOQ)	0.035 – 0.18
27-OH-Chl	1.0 – 5.0 (>LOD < LOQ)	0.035 – 0.18
7α-OH-Chl (P1, P2)* + 7β-OH-Chl (P1, P2)*	47.8 ± 2.0	1.67 ± 0.07
7-ketochl	5.0 ± 1.1	0.21 ± 0.04

* P1 = protomer 1 and P2 = protomer 2

Feasibility of ultra-performance liquid chromatography–ion mobility–time-of-flight mass spectrometry in analyzing oxysterols

Petri Kylli[a], Thomas Hankemeier[b,d], Risto Kostiainen[a,*]

[a] Division of Pharmaceutical Chemistry and Technology, Faculty of Pharmacy, University of Helsinki, P.O. Box 56, FI-00014, Finland (linda.ahonen@helsinki.fi, risto.kostiainen@helsinki.fi, petri.kylli@helsinki.fi)

[b] Division of Analytical Biosciences, Leiden Academic Centre for Drug Research, Leiden University, P.O. Box 9502, 2300 RA Leiden, The Netherlands (hankemeier@lacdr.leidenuniv.nl)

[d] Netherlands Metabolomics Centre, Leiden University, P.O. Box 9502, 22300 RA Leiden, The Netherlands (hankemeier@lacdr.leidenuniv.nl)

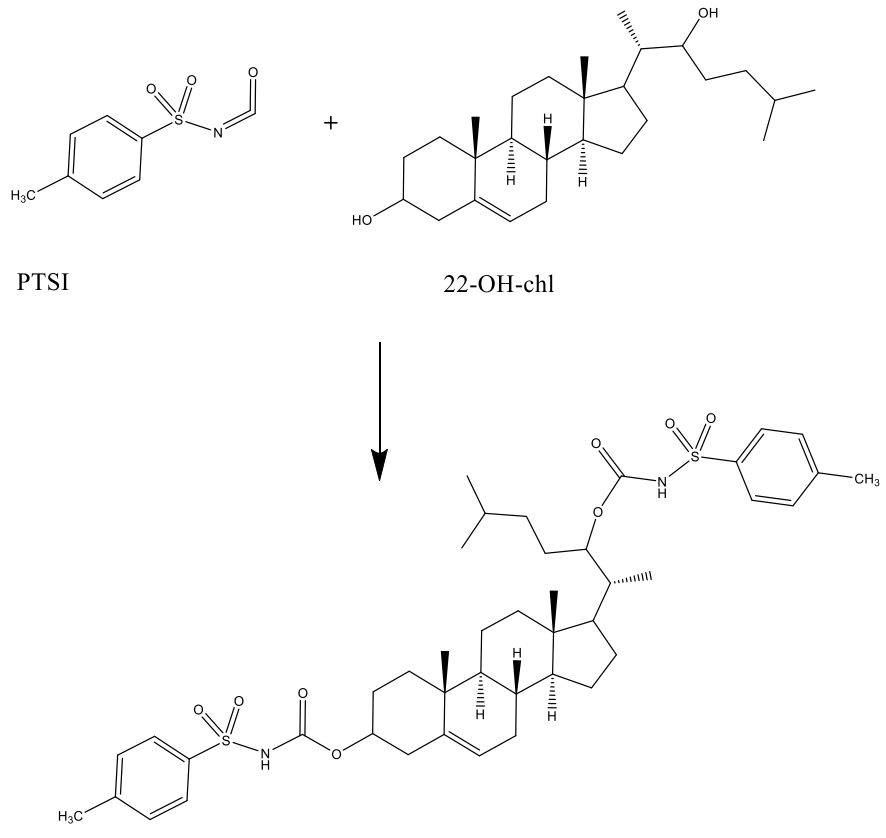

Figure S1. Example of derivatization reaction.

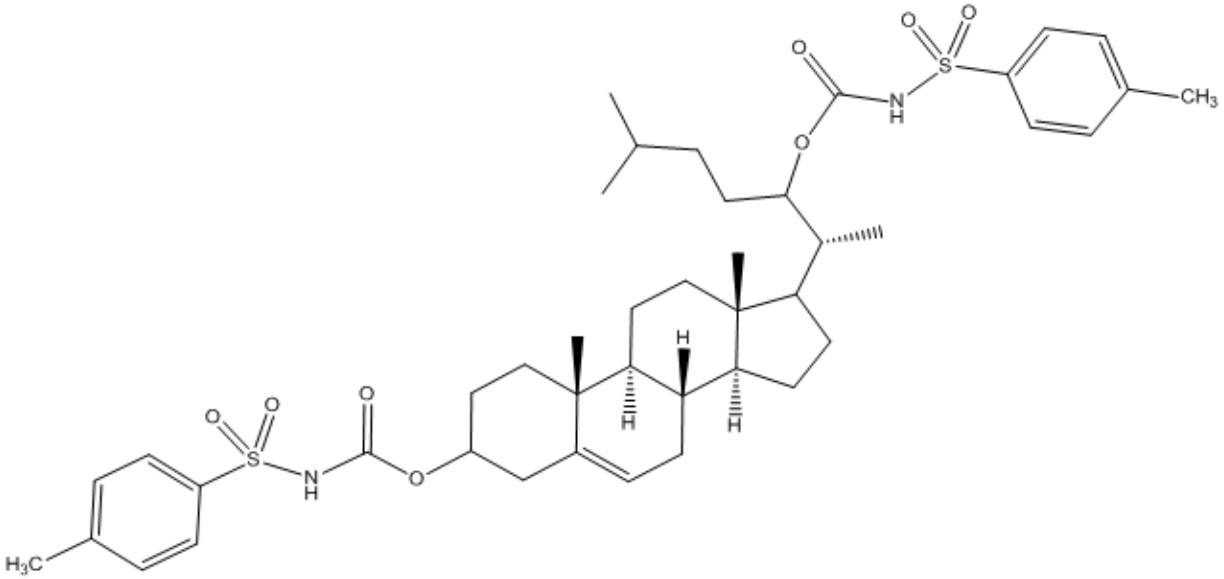

22-OH-Chl
Exact mass 796.3791

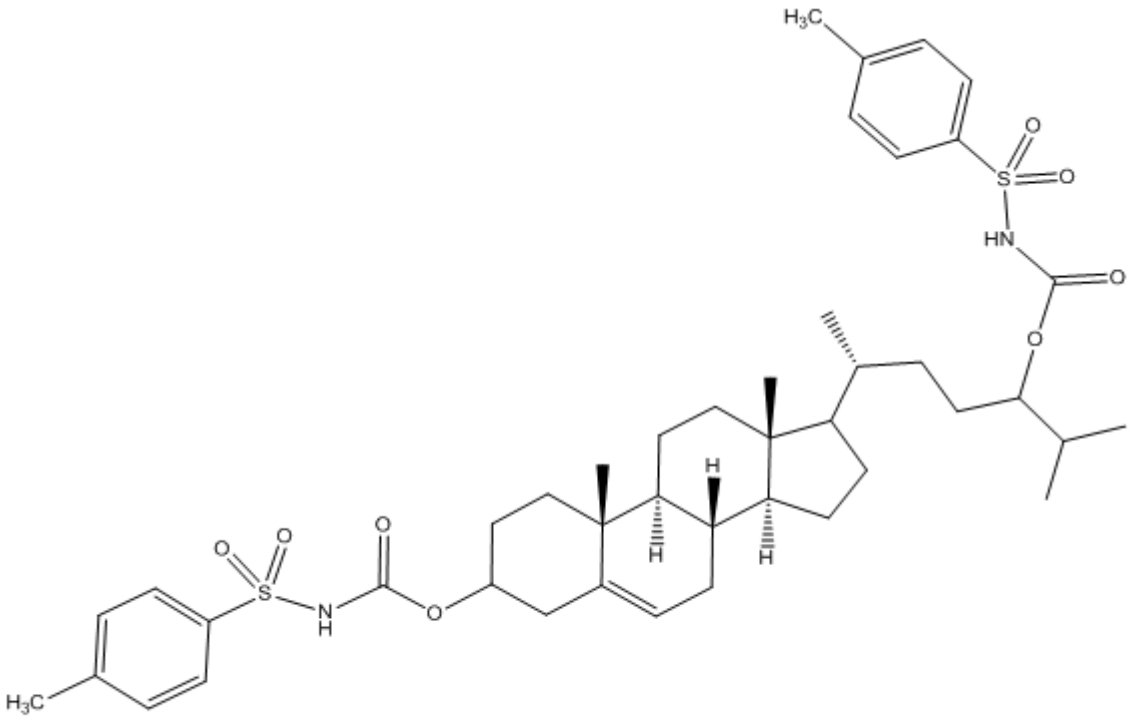

24*(S)*-OH-Chl
Exact mass 796.3791

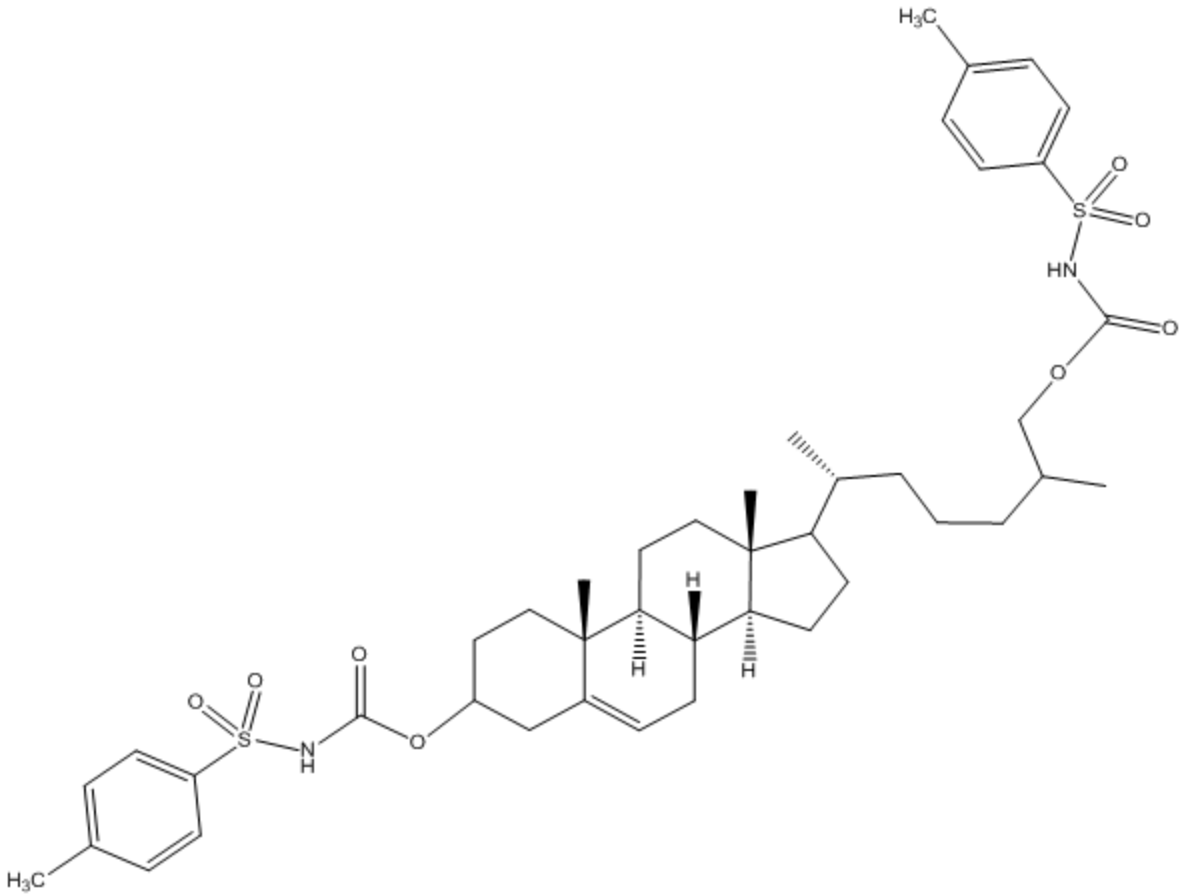

27-OH-Chl
Exact mass 796.3791

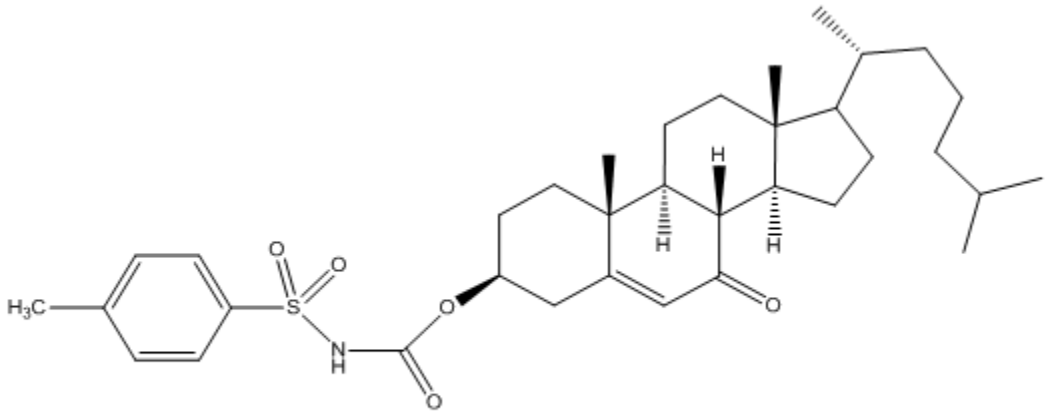

7-ketochl
Exact mass 597.3488

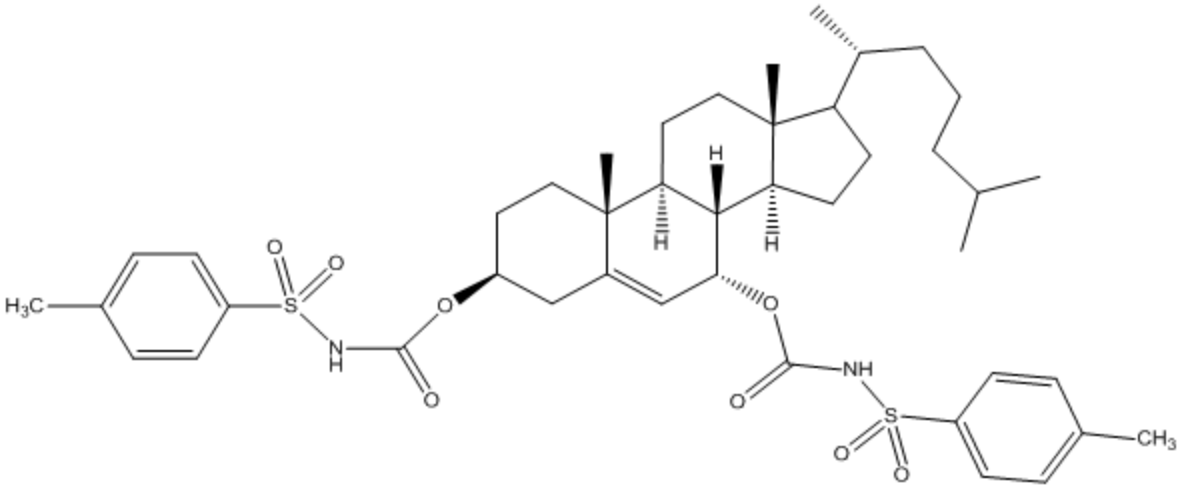

7α-OH-Chl
Exact mass 796.3791

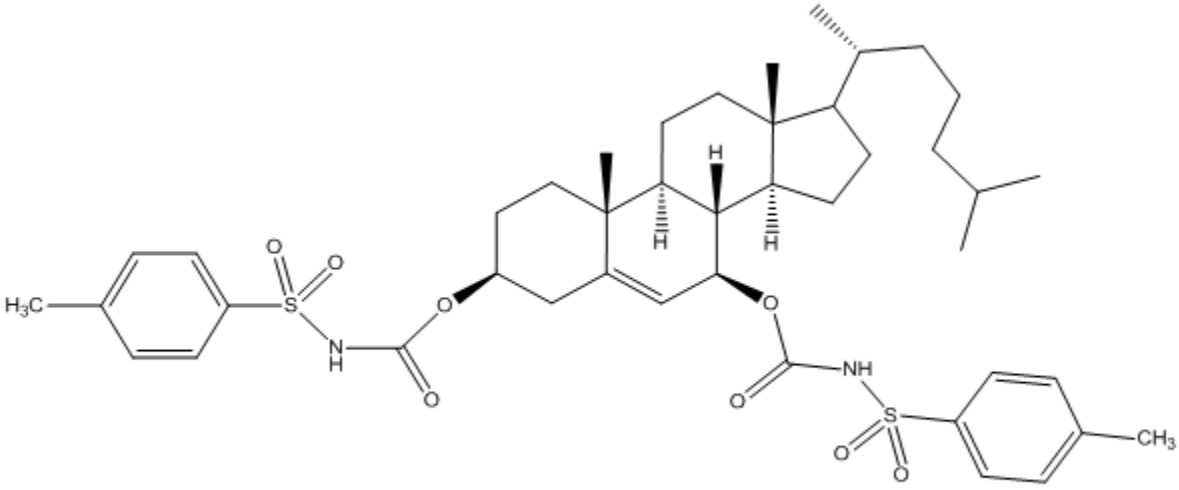

7β-OH-Chl
Exact mass 796.3791

Figure S2. Structures of PTSI-derivatized oxysterols.

Peak-to-peak resolution ($R_{P\text{-}P}$) of two adjacent peaks were calculated using the following equations:

$$R_{P-P} = 0.589\, R_P \frac{\alpha-1}{\alpha}$$

where R_p is a the ratio between the drift time (dt) and peak width half height ($w_{½}$),

$$R_P = \frac{dt}{w_{1/2}}$$

and α is the ratio between adjacent peaks:

$$\alpha = \frac{dt_b}{dt_a}$$

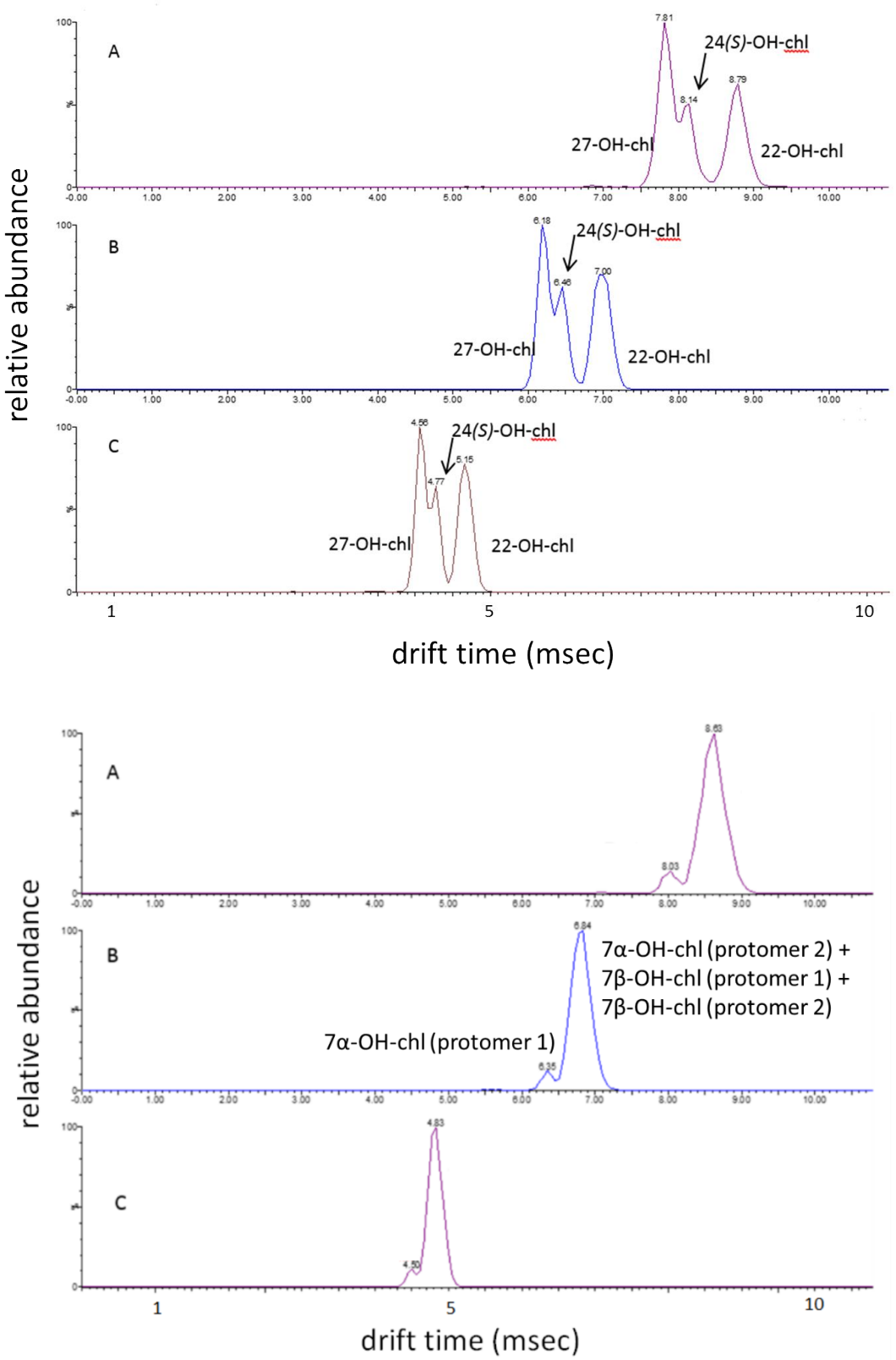

Figure S3. Selected ion mobility responses of the $[M-H]^-$ ions (*m/z* 795.3718 +/- 10 ppm) of the PTSI-derivatized 22-, 24(*S*)- and 27-OH-cholesterol and 7α-OH- and 7β-OH-cholesterol at drift gas (N_2) pressures of 2.5 (A), 3.0 (B), and 3.5 (C) bar.

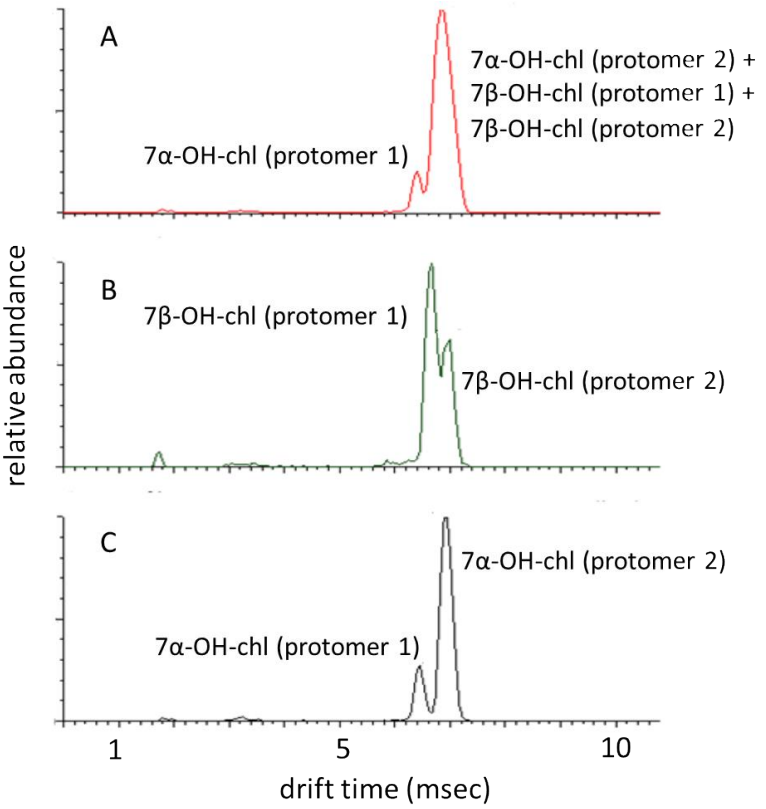

Figure S4. Selected ion mobility responses of the $[M-H]^-$ ions (*m/z* 795.3718 +/- 10 ppm) of the PTSI-derivatized 7α-OH- and 7β-OH-cholesterol as a mixture (A), 7β-OH-cholesterol (B), and 7α-OH- cholesterol (C) at drift gas (N_2) pressure of 3.0 bar.